

# Enantioselective Hydrolysis of Some 2-Aryloxyalkanoic Acid Methyl Esters and Isosteric Analogues Using a Penicillin G Acylase-Based HPLC Monolithic Silica Column

Gabriella Massolini,<sup>\*,†</sup> Enrica Calleri,<sup>†</sup> Antonio Lavecchia,<sup>‡</sup> Fulvio Loiodice,<sup>§</sup> Dieter Lubda,<sup>||</sup> Caterina Temporini,<sup>†</sup> Giuseppe Fracchiolla,<sup>§</sup> Paolo Tortorella,<sup>⊥</sup> Ettore Novellino,<sup>‡</sup> and Gabriele Caccialanza<sup>†</sup>

Dipartimento di Chimica Farmaceutica, Università di Pavia, Via Taramelli 12, I-27100 Pavia, Italy, Dipartimento di Chimica Farmaceutica e Tossicologica, Università di Napoli "Federico II", Via Domenico Montesano, 49, I-80131 Napoli, Italy, Dipartimento Farmaco-Chimico, Via Orabona 4, I-70126 Bari, Italy, LSP R&D MDA, Merck KGaA, Frankfurter Str 250, D-64293 Darmstadt, Germany, and Dipartimento di Scienze del Farmaco, Università "G.D'Annunzio", Via dei Vestini, I-66100 Chieti, Italy

**A technique based on liquid chromatography has been developed to facilitate studies of enantioselectivity in penicillin G acylase (PGA)-catalyzed hydrolysis of some 2-aryloxyalkanoic acid methyl esters and isosteric analogues. PGA was covalently immobilized on an aminopropyl monolithic silica support to create an immobilized HPLC-enzyme reactor. Two sets of experimental data were drawn to calculate the enantioselectivity (*E*) of the kinetically controlled enantiomer-differentiating reaction, the degree of substrate conversion and the enantiomeric excess of the product. The developed enzymatic reactor was coupled through a switching valve to an achiral analytical column for separation and quantitation of the hydrolysis products. The enantiomeric excess was determined *off-line* on a PGA-chiral stationary phase. In this way, highly precise *E* values were determined. A computational study related to the hydrolysis of the considered racemic esters was also carried out in order to unambiguously clarify both the substrate specificity and the enantioselectivity displayed by PGA.**

Penicillin G acylase (PGA) is best known for the regioselective hydrolysis of the side chains of penicillin G and penicillin V in the commercial synthesis of 6-aminopenicillanic acid.<sup>1</sup> PGA selectivity toward substrates other than penicillin G has attracted the interest of researchers since it has been demonstrated that this enzyme is able to hydrolyze a large variety of amides and esters containing aromatic acyl moieties.<sup>2–5</sup> The enzyme shows a

strong affinity for the phenyl–acetyl moiety and a high tolerance as far as the rest of the molecule is concerned. This capacity has been used advantageously to achieve moderate-to-excellent stereochemical discrimination between corresponding enantiomers in the hydrolytic cleavage of the phenyl–acetyl group from  $\alpha$ -aminoalkylphosphoric acids,  $\alpha$ -,  $\beta$ -, and  $\gamma$ -amino carboxylic acids, sugar, amines, peptides, and esters of phenylacetic acid. However, a detailed understanding of the structural factors affecting the rate and stereochemistry of these reactions is still lacking, and a deeper knowledge of the enzyme's specificity could facilitate the engineering of this catalyst, enhancing its potential for chemical and industrial applications.

Recently, the X-ray structures of PGA complexed with a series of phenylacetic acid analogues<sup>6</sup> and with penicillin G/penicillin G sulfoxide ligands<sup>7</sup> have been solved, shedding light on the functional properties of PGA and on its catalytic mechanism. PGA belongs to the newly recognized structural superfamily of N-terminal nucleophile (Ntn) amidohydrolases.<sup>8</sup> Other Ntn hydrolases identified so far are aspartylglucosaminidase (AGA),<sup>9</sup> proteasome (PRO),<sup>10</sup> and glutamine-PRPP-amidotransferase (GAT).<sup>11</sup> The enzymes of the superfamily share similar three-dimensional folds and function analogously. The architecture of their active sites is also similar with corresponding catalytic elements arranged in analogous ways.<sup>8</sup> On the basis of the X-ray structures and biochemical studies, the well-known serine protease-like catalytic

- (4) Rossi, D.; Romeo, A.; Lucente, G. *J. Org. Chem.* **1978**, *43*, 2576–2581.
- (5) Baldaro, E.; D'Arrigo, P.; Pedrocchi-Fantoni, G.; Rosell, C. M.; Servi, S.; Tagliani, A.; Terreni, M. *Tetrahedron Asymmetry* **1993**, *4*, 1031–1034.
- (6) Done, S. H.; Brannigan, J. A.; Moody, P. C. E.; Hubbard, R. E. *J. Mol. Biol.* **1998**, *284*, 463–475.
- (7) McVey, C. E.; Walsh, M. A.; Dodson, G. G.; Wilson, K. S.; Brannigan, J. A. *J. Mol. Biol.* **2001**, *313*, 139–150.
- (8) Brannigan, J. A.; Dodson, G.; Duggleby, H. J.; Moody, P. C. E.; Smith, J. L.; Tomchick, D. R.; Murzin, A. G. *Nature* **1995**, *378*, 416–419.
- (9) Mononen, I.; Fischer, K. J.; Kaartinen, V.; Aronson, N. N. *FASEB J.* **1993**, *7*, 1247–1256.
- (10) Löwe, J.; Stock, D.; Jap, B.; Zwickl, P.; Baumeister, W.; Huber, R. *Science* **1995**, *268*, 533–539.
- (11) Smith, J. L.; Zaluzec, E. J.; Wery, J. P.; Niu, L.; Switzer, R. L.; Zalkin, H.; Satow, Y. *Science* **1994**, *264*, 1427–1433.

\* Corresponding author: (fax) +39 382 422975; (e-mail) g.massolini@unipv.it.

<sup>†</sup> Università di Pavia.

<sup>‡</sup> Università di Napoli "Federico II".

<sup>§</sup> Dipartimento Farmaco-Chimico.

<sup>||</sup> Merck KGaA.

<sup>⊥</sup> Università "G.D'Annunzio".

- (1) Duggleby, H. J.; Tolley, S. P.; Hill, C. P.; Dodson, E. J.; Moody, P. C. E. *Nature* **1995**, *373*, 264–268.
- (2) Fuganti, C.; Rosell, C. M.; Servi, S.; Tagliani, A.; Terreni, M. *Tetrahedron Asymmetry* **1992**, *3*, 383–386.
- (3) Rossi, D.; Calcagni, A.; Romeo, A. *J. Org. Chem.* **1979**, *44*, 2222–2225.

mechanism<sup>11–16</sup> involving Ntn amidohydrolases<sup>1,10</sup> has been demonstrated.

A novel feature of the catalytic machineries of the Ntn amidohydrolases is that the nucleophile, which attacks the carbonyl carbon of the scissile amide or ester bond, and the base, which facilitates the attack by accepting the proton from the nucleophile, are located in the same N-terminal amino acid. In the case of PGA, the nucleophilic residue is the N-terminal serine, in the case of AGA and PRO, threonine, and in the case of GAT, the N-terminal cysteine. The neutral R-amino group of the N-terminal amino acid, corresponding to histidine of the serine proteases, is thought to act as a base in the catalytic mechanisms of Ntn amidohydrolases. This is supported by the fact that the optimum pH of the rate of the catalytic reactions is between 7 and 9 for these enzymes.<sup>1,17,18</sup> The oxyanion binding site (i.e., oxyanion hole) has also been identified from the structures of Ntn amidohydrolases.

In the present paper, a series of nine racemic 2-aryloxyalkanoic acid methyl esters and isosteric analogues were considered in order to study the structural effects on the rate and enantioselectivity of the esterolytic reactions catalyzed by immobilized PGA.

Studies of such hydrolytic reactions are usually carried out "in batch" and these procedures are often followed by additional steps involving substrate and product extraction and *off-line* quantitation of the hydrolysis products. This multistep process is time-consuming and may yield unreproducible results; therefore, an immobilized PGA reactor for *on-line* conversion of substrates was applied. This approach allows the direct evaluation of the unreacted substrate as well as the two product enantiomers.

In this work, PGA was immobilized on monolithic chromatographic support. These innovative materials are based on a development of Nakanishi and Soga,<sup>19</sup> who used a new sol-gel process for the preparation of monolithic silica columns with a bimodal pore structure (i.e., with throughpores and mesopores). Tanaka et al.<sup>20,21</sup> and Cabrera et al.<sup>22</sup> demonstrated that this method allows the preparation of chromatographic columns with high efficiencies and low column back pressures. Due to their properties concerning the fast mass transfer between the substance within the eluent and the active sites inside the skeleton of the monolithic silica support, these materials seem to be an ideal material for the immobilization of enzymes and the fast conversion of substrates. Monoliths differ from the conventional columns as regards their hydrodynamic properties especially since

they have the same fast mass transfer as 3- $\mu\text{m}$  particulate materials (as shown by comparing the H/U behavior of comparable columns), but at the same time they offer a low-pressure drop as  $\sim 15\text{-}\mu\text{m}$  particles. Both properties play a crucial role in chromatography performance and speed.

The developed enzymatically active monolithic reactor was coupled through a switching valve to an analytical column for on-line separation and quantitation of the hydrolysis product to calculate the total ester hydrolysis. The enantiomeric excess of the product was calculated *off-line* on a CSP utilizing immobilized penicillin G acylase (PGA-CSP).

With the aim of shedding light on the experimentally observed substrate specificity, a computational study was also undertaken. The recognition process between PGA and its substrates was simulated through the docking and molecular dynamics of the studied compounds inside the active site of the enzyme.

## EXPERIMENTAL SECTION

**Chemicals.** Penicillin G acylase crude extract from *Escherichia coli* ATCC 11105 (EC 3.5.1.11) was kindly donated by Recordati (Milan, Italy). *N,N*-Disuccinimidyl carbonate (DSC), Bradford reagent, penicillin G potassium salt, phenylacetic acid (PAA), and 6-aminopenicillanic acid (6-APA) were purchased from Sigma-Aldrich (Milan, Italy). Potassium dihydrogen phosphate and dipotassium hydrogen phosphate used for the preparation of the mobile phases were of analytical grade and purchased from Merck (Darmstadt, Germany). Acetonitrile, methanol, and 1-propanol were from Carlo Erba (Milan, Italy). Water was deionized by passing through a Direct-Q (Millipore) system (Millipore, Bedford, MA). Chromolith Performance NH<sub>2</sub> (2- $\mu\text{m}$  macropores, mesopore size 13 nm), (10 cm  $\times$  0.46 (i.d.) cm) research sample was from Merck. Zorbax RX-C8 column (15 cm  $\times$  0.46 (i.d.) cm) was purchased from Agilent Technologies.

Racemic acids were prepared according to our previous papers<sup>23,24</sup> and quantitatively converted to methyl esters **1–9** using a solution of diazomethane (*caution!! diazomethane is explosive, toxic, and carcinogenic*) in diethyl ether. Mass and NMR spectra were consistent with the identity and purity of the so obtained compounds. The methyl esters' chemical structures are listed in Table 1. The pure (+)-enantiomers of the considered acid racemates were prepared<sup>25</sup> and used for the determination of the enantiomeric elution order on PGA-chiral stationary phase.<sup>26</sup>

**Apparatus. Titration.** Titration was performed by means of 718 STAT Titrino from Metrohm Italiana (Saronno, VA, Italy). **Chromatography.** Chromatographic experiments were performed with three modular systems. The systems were connected to HPLC ChemStation, (Revision A.04.01). All the chromatographic experiments were carried out at 25 °C. **System 1.** System 1 consisted of a Hewlett-Packard HP1050 chromatographic pump (Palo Alto, CA), a Rheodyne sample valve (20- $\mu\text{L}$  loop), and the enzyme reactor. **System 2.** System 2 consisted of a Hewlett-Packard

(12) Warshel, A.; Naray-Szabo, G.; Sussman, F.; Hwang, J.-K. *Biochemistry* **1989**, *28*, 3629–3637.

(13) Daggett, V.; Schröder, S.; Kollman, P. *J. Am. Chem. Soc.* **1991**, *113*, 8926–8935.

(14) Warshel, A.; Russell, S. *J. Am. Chem. Soc.* **1986**, *108*, 6569–6579.

(15) Nakagawa, S.; Yu, H.-A.; Karplus, M.; Umeyama, H. *Proteins* **1993**, *16*, 172–194.

(16) Kraut, J. *Annu. Rev. Biochem.* **1977**, *46*, 331–358.

(17) Kaartinen, V.; Williams, J. C.; Tomich, J.; Yates, J. R.; Hood, L. E.; Mononen, I. *J. Biol. Chem.* **1991**, *266*, 5860–5869.

(18) Seemüller, E.; Lupas, A.; Zühl, F.; Zwickl, P.; Baumeister, W. *FEBS Lett.* **1995**, *359*, 173–178.

(19) Nakanishi, K.; Soga, N. *J. Non Cryst. Solids* **1992**, *139*, 1–13, 14–24.

(20) Tanaka, N.; Kobayashi, H.; Ishizuka, N.; Minakuchi, H.; Nakanishi, K.; Hosoya, K.; Ikegami, T. *J. Chromatogr., A* **2002**, *965*, 35–49.

(21) Minakuchi, H.; Nakanishi, K.; Soga, N.; Ishizuka, N.; Tanaka, N. *Anal. Chem.* **1996**, *68*, 3498–3501.

(22) Cabrera, K.; Lubda, D.; Eggenweiler, H.-M.; Minakuchi, H.; Nakanishi, K. *J. High Resolut. Chromatogr.* **2000**, *23*, 99–104.

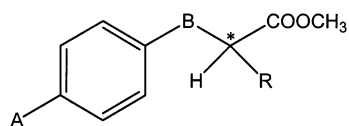
(23) Romstedt, K. J.; Lei, L.-P.; Feller, D. R.; Witiak, D. T.; Loiodice, F.; Tortorella, V. *Farmaco* **1996**, *51*, 107–114.

(24) Bettoni, G.; Ferorelli, S.; Loiodice, F.; Tangari, N.; Tortorella, V.; Gasparrini, F.; Misiti, D.; Villani, C. *Chirality* **1992**, *4*, 193–203.

(25) Ferorelli, S.; Loiodice, F.; Tortorella, V.; Amoroso, R.; Bettoni, G.; Conte-Camerino, D.; De Luca, A. *Farmaco* **1997**, *52*, 367–374.

(26) Calleri, E.; Massolini, G.; Loiodice, F.; Fracchiolla, G.; Temporini, C.; Felix, G.; Tortorella, P.; Caccialanza, G. *J. Chromatogr., A* **2002**, *958*, 131–140.

Table 1. Chemical Structures of the Substrates Used in the Study



racemate	A	B	R
<b>1</b>	Cl	O	CH <sub>3</sub>
<b>2</b>	Cl	O	C <sub>2</sub> H <sub>5</sub>
<b>3</b>	Cl	O	C <sub>6</sub> H <sub>5</sub>
<b>4</b>	Cl	S	CH <sub>3</sub>
<b>5</b>	Cl	NH	CH <sub>3</sub>
<b>6</b>	Cl	CH <sub>2</sub>	CH <sub>3</sub>
<b>7</b>	Br	O	CH <sub>3</sub>
<b>8</b>	F	O	CH <sub>3</sub>
<b>9</b>	CH <sub>3</sub>	O	CH <sub>3</sub>

HP 1100 liquid chromatograph with a Rheodyne sample valve (20- $\mu$ L loop) equipped with a Hewlett-Packard HP 1100 variable-wavelength detector, a HP 1100 thermostat, and the Zorbax RX-C8 column. *System 1–2.* Systems 1 and 2 could be used independently or the eluent from system 1 could be directed onto system 2 through a HP six-port switching valve as shown in Figure 1. The UV detector could be connected to system 1 or to system 2 through a second switching valve (detector selector valve). *System 3.* System 3 consisted of a Hewlett-Packard HP 1100 liquid chromatograph with a Rheodyne sample valve (20- $\mu$ L loop) equipped with a Hewlett-Packard HP 1100 diode-array detector, a HP 1100 thermostat, and a PGA-epoxide chiral stationary phase (15 cm  $\times$  0.46 (i.d.) cm). The mobile phase was 120 mM phosphate buffer (pH 7.0). The flow rate was maintained at 0.8 mL/min and the detection was performed at 225 nm.

**Methods.** *Column-Switching Setup.* A schematic drawing of the column-switching system (system 1–2) is given in Figure 1.

Step 1 (0–1.2 min, valve 1 in position A): the substrates were loaded on the enzymatic column (system 1); 50 mM phosphate buffer (pH 7.0) at a flow rate of 0.8 mL/min was used as eluent (pump 1).

Step 2 (1.2–14.0 min, valve 1 in position B): valve 1 was switched to position B and the analytes (products and unreacted substrate) were flushed and focused directly to the reversed-phase analytical column (pump 1) using 50 mM phosphate buffer (pH 7.0) as mobile phase at a flow rate of 0.8 mL/min.

Step 3 (14.0–39.0 min, valve 1 position A): the valve was then switched back to its original position for separation of products and unreacted substrate on Zorbax RX-C8 (system 2). The following mobile-phase gradient was applied (pump 2): 50 mM phosphate buffer (pH 7.0)–methanol (60:40) for the first 10 min, step gradient to 50 mM phosphate buffer (pH 7.0)–methanol (40:60) at 10.01 min, and return to the starting condition at 25 min. The flow rate was 1.0 mL/min, and the detection was performed at 225 nm.

A representative chromatogram obtained from the chromatography of ester **6** on the coupled PGA-column/analytical column is presented in Figure 2.

*Analytical Procedure.* Stock solutions of each racemic substrate were prepared in 1-propanol at a concentration of 10 mM and then diluted with 50 mM phosphate buffer (pH 7.0) to a final concentra-

tion of 5 mM. The substrate solutions were injected into the coupled LC system. The rates of substrate conversion (C) were calculated from the peak areas of unreacted esters. Standard curves for the substrates were linear over the concentration range of 0.1–5 mM corresponding to 2 and 100% of conversion.

The product of the enzymatic hydrolysis was collected from the analytical column in a 1-mL volumetric flask and directly injected into system 3 for chiral resolution and determination of the product enantiomeric excess (ee<sub>p</sub>). For the compound with the highest enantioselectivity (compound **3**) the lowest level of the *R* enantiomer was determined. The limit of quantitation (LOQ) for the *R* enantiomer was  $\sim$ 0.05% (w/w) at a signal-to-noise ratio of 10. A typical chromatogram of the *S* enantiomer of the acid corresponding to ester **3** spiked with 0.05% *R* enantiomer is presented in Figure 3.

*PGA Immobilization.* PGA was covalently immobilized on a Chromolith-NH<sub>2</sub> column. The immobilization of the enzyme via amino groups was carried out according to a previously described procedure following the in situ method.<sup>27,28</sup> A total of 2.24 g of DSC was dissolved in 100 mL of acetonitrile, and the resulting solution was continuously circulated for 18 h at 0.5 mL/min through the column previously equilibrated with the same solvent. The column was then washed at the same flow rate, first with 60 mL of acetonitrile and then with water and with 60 mL of 1 mM phosphate buffer (pH 7.0). A total of 300 mg of PGA was dissolved in 100 mL of 1 mM phosphate buffer (pH 7.0) and the enzyme solution continuously circulated at 0.5 mL/min for 24 h. The flow was inverted every 15 min in the first hour and then every 30 min in the following 3 h. After 24 h, the column was washed with 200 mL of water, 200 mL of a 0.5 M solution of NaCl, and finally with 100 mL of a 0.2 M glycine solution to block the remaining activated groups and equilibrated with a 50 mM solution of phosphate buffer (pH 7.0).

The amount of immobilized units was calculated from the difference between the initial and the final enzymatic activity of the enzymatic solution. The hydrolysis of penicillin G potassium salt has been used as a standard assay for the determination of the catalytic activity of the enzyme. The hydrolysis was carried out in 20 mL of a 100 mM penicillin G solution in 50 mM phosphate buffer (pH 7.0) and the PAA produced was titrated with 0.1 M NaOH with automatic pH correction. The experiments were carried out at room temperature. The enzymatic activity was measured as international units (U), equivalent to micromoles of penicillin G hydrolyzed per minute. The amount of immobilized units were found to be 1406 U, corresponding to 58.58 mg of enzyme as determined with Bradford reagent. When not in use, the columns were stored at 4 °C in a solution of 0.01% sodium azide (w/v).

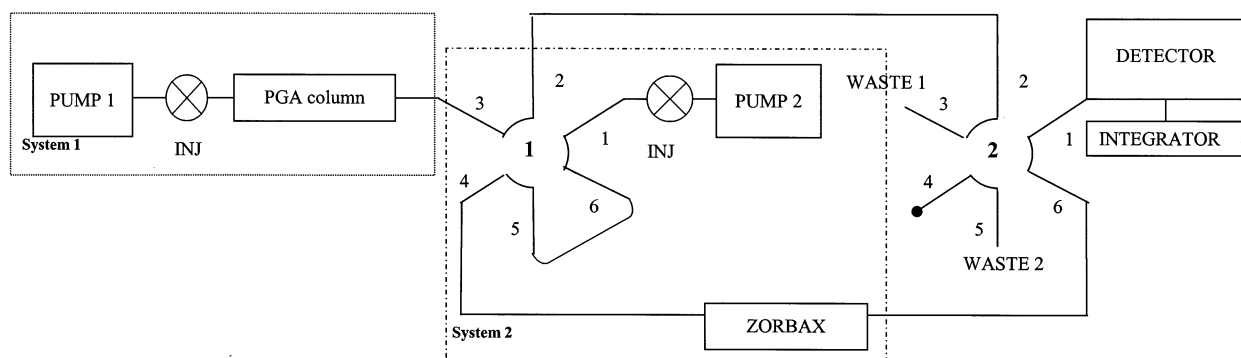
*PGA Column Activity Determination.* The hydrolysis of penicillin G potassium salt has been used as a standard assay for the determination of the catalytic activity of the enzyme in the immobilized form using chromatographic system 1.<sup>29</sup> The enzyme column was equilibrated for 30 min with 50 mM phosphate buffer (pH 7.0). A 20- $\mu$ L aliquot of penicillin G diluted in the same buffer

(27) Massolini, G.; Calleri, E.; De Lorenzi, E.; Pregolato, M.; Terreni, M.; Felix, G.; Gandini, C. *J. Chromatogr., A* **2001**, *921*, 147–160.

(28) Felix, G.; Descorps, V. *Chromatographia* **1999**, *49*, 595–605.

(29) Andrisano, V.; Bartolini, M.; Gotti, R.; Cavrini, V.; Felix, G. *J. Chromatogr., B* **2001**, *753*, 375–383.

**POSITION A**



**POSITION B**

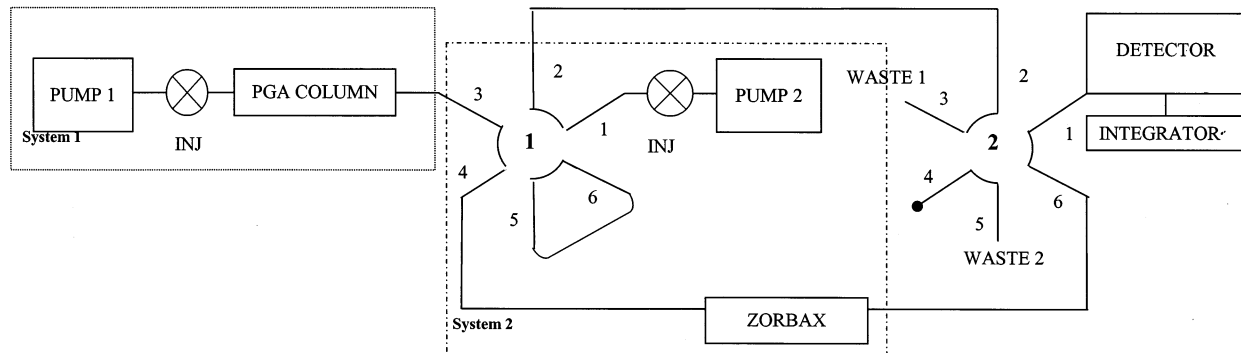


Figure 1. Chromatographic system coupling the enzyme column with the reversed-phase analytical column. The substrate is loaded onto the enzyme column using position A; the product and the unreacted substrate are switched to the analytical column using position B; the conversion percentage is measured on the analytical column using position A. 1, switching valve; 2, detector selector valve.

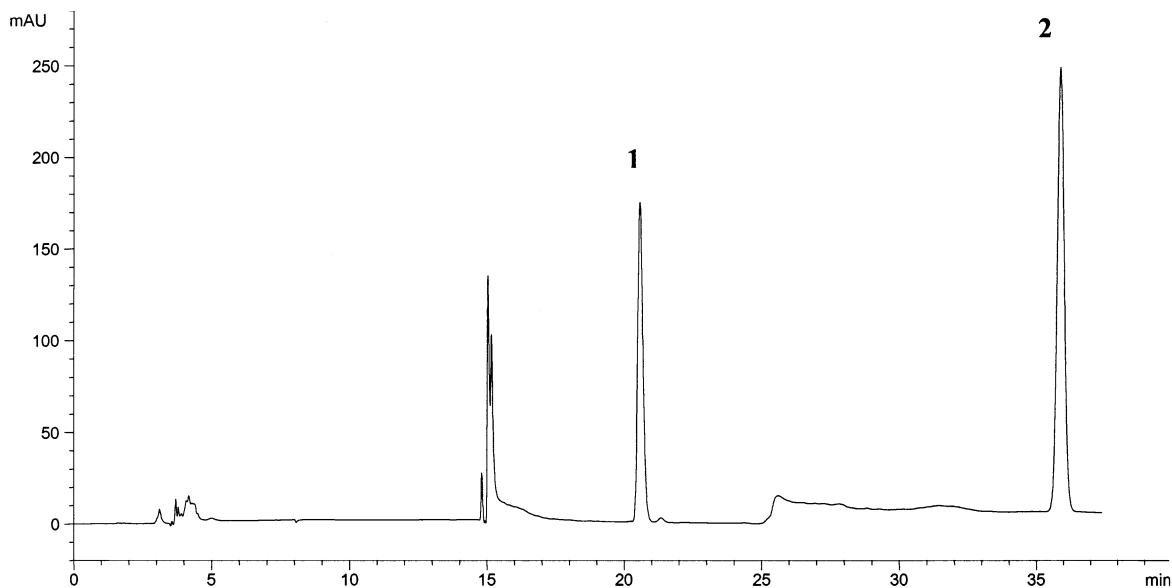


Figure 2. Chromatogram showing the separation of the product from the unreacted substrate racemate 6 obtained on-line with the coupled system. See text for experimental conditions. Peak 1, acidic product; peak 2, unreacted substrate.

solution, concentration range between 0.1 and 4 M, was injected onto the HPLC system with a flow rate of 0.5 mL/min and UV detection at 225 nm. Each concentration was injected in duplicate. The species eluted from the PGA column were contained in the first 3-mL fraction of each eluate (6 min). Each fraction was collected in a 10-mL volumetric flask (dilution factor,  $df = 10/3$ ) adjusting the volume with 50 mM phosphate buffer (pH 7.0). Each

solution was injected off-line in system 2. The mobile phase employed was 50 mM phosphate buffer (pH 7.0)–methanol (70:30). Flow rate was 0.8 mL/min, and the detector was set at 225 nm. The chromatographic retention factors were 0.17 for 6-APA, 0.60 for phenylacetic acid, and 2.55 for penicillin G. The amount of PAA from PGA-catalyzed hydrolysis was found to be dependent on the concentration of injected penicillin G. The Michaelis–

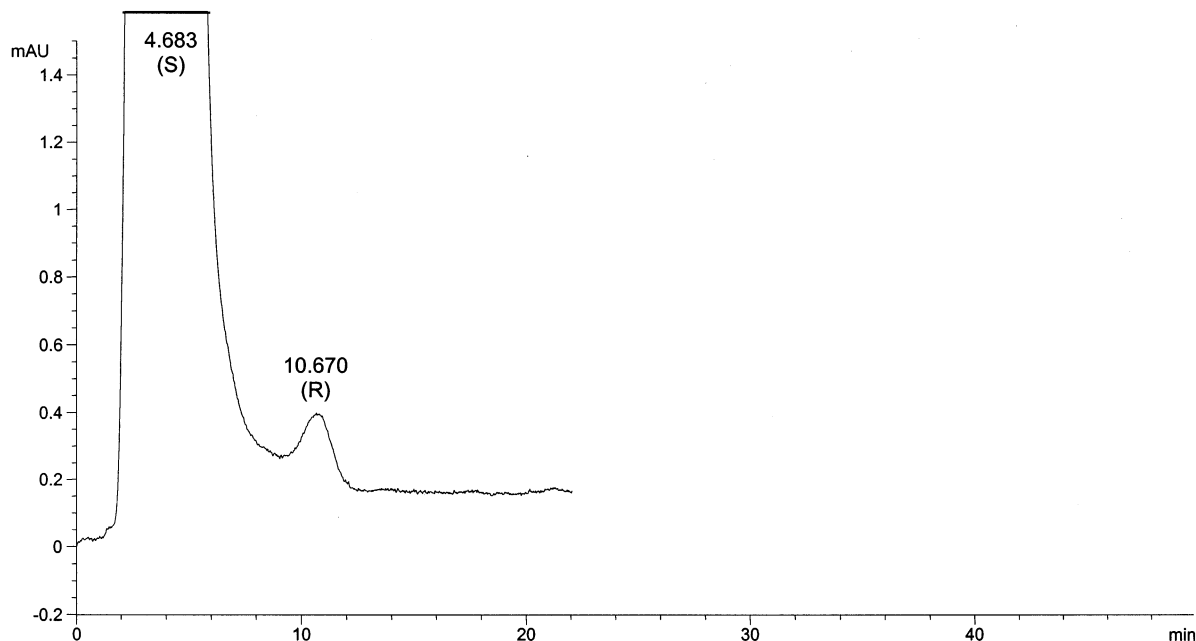


Figure 3. Typical chromatogram of the *S* enantiomer of the acid corresponding to ester **3** containing 0.05% *R* enantiomer.

Menten trend was found by plotting the rate of enzymatic reaction against the substrate concentration [S].

The rate of the enzymatic reaction  $V$  expressed as ( $\Delta$ area PAA/min) was calculated by

$$V (\Delta\text{area}/\text{min}) = \frac{\text{area (PAA)} \times df/\text{time (min)}}{\text{area (PAA)} \times (10/3)/6}$$

To obtain estimate of the  $V_{\text{max}}$ , Lineweaver and Burk reciprocal plots of  $1/V$  versus  $1/[S]$  were constructed.

To calculate the units (U) of immobilized enzyme, the following equation was used:

$$U (\mu\text{mol}/\text{min}) = \frac{[(\Delta\text{area}/\text{min})_{\text{max}}/\text{extinction coefficient}] \times \text{column void volume (mL)} \times 10^3}{\text{area (PAA)} \times (10/3)/6}$$

where one unit (U) is the amount of enzyme that hydrolyses 1  $\mu\text{mol}$  of penicillin G in 1 min.

To determine the phenylacetic acid extinction coefficient for concentration assessment (area of a 1 M concentration of PAA), increasing concentrations of phenylacetic acid were injected onto the enzyme column. Four calibration solutions in the range between 0.1 and 4 M were prepared, and each solution was injected twice. For each injected concentration, the PAA area was determined by collecting 10 mL of each eluate from the enzyme column in a volumetric flask; each solution was then injected off-line on the RX-C8 Zorbax, measuring the area at 225 nm and plotting against the corresponding PAA concentration. A linear correlation ( $r^2 = 0.999$ ) was found, providing the extinction coefficient value.

The amount of active immobilized enzyme was found to be  $1420.09 \pm 29.5$  units, this result is comparable to the value of immobilized units (1406 U); therefore, all the immobilized enzyme was found to be active after the immobilization procedure.

**Calculations.** The retention factor ( $k$ ) was calculated using the equation  $k = (t_r/t_0) - 1$ , where  $t_r$  is the retention time of the

analyte and  $t_0$  is the retention time of an unretained compound; in this study,  $t_0$  was calculated from the first disturbance of the baseline after injection. The void volume was calculated from the first disturbance of the baseline after injection.

The product enantiomeric excess was calculated as follows:

$$ee_p = \frac{(x_1 - x_2)}{x_1 + x_2} \quad (1)$$

where  $x_1$  and  $x_2$  denote the concentrations of the two acidic enantiomers separated on the chiral stationary phase.

The enantioselectivity  $E$ , for an irreversible enantiomer-differentiating enzyme-catalyzed hydrolysis, is expressed as

$$E = \frac{\ln[1 - C(1 + ee_p)]}{\ln[1 - C(1 - ee_p)]} \quad (2)$$

where  $C$  is the degree of substrate conversion, or conversion factor.<sup>30</sup>

**Modeling of Transition-State Analogues in PGA.** All modeling was done with the Sybyl software package,<sup>31</sup> running on a Silicon Graphics R10000 workstation. Energy minimizations and molecular dynamics calculations were done using the Tripos force field<sup>32</sup> including the electrostatic contribution. Atom-centered partial charges were calculated according to the Gasteiger–Hückel method.<sup>33,34</sup>

We used a distance-dependent dielectric constant of 4.0 and scaled the 1–4 van der Waals interactions by 50%. The distance-dependent dielectric constant damps long-range electrostatic interactions and thus compensates for the lack of explicit solva-

(30) Chen, C. S.; Fujimoto, Y.; Girdaukas, G.; Sih, C. J. *J. Am. Chem. Soc.* **1982**, *104*, 7294–7299.

(31) *Sybyl Molecular Modelling System* (version 6.8); Tripos Inc.: St. Louis, MO.

(32) Vinter, J. G.; Davis, A.; Saunders, M. R. *J. Comput.-Aided Mol. Des.* **1987**, *1*, 31–55.

(33) Gasteiger, J.; Marsili, M. *Tetrahedron* **1980**, *36*, 3219–3228.

(34) Purcell, V. P.; Singer, J. A. *J. Chem. Eng. Data* **1967**, *12*, 235–246.

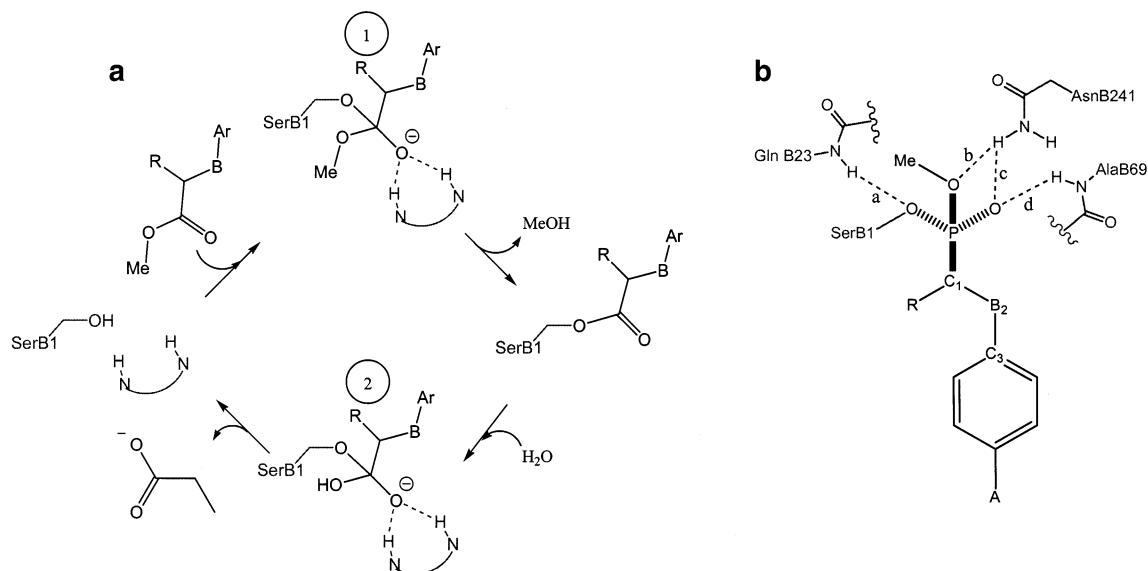


Figure 4. Intermediates and their analogues in the PGA-catalyzed hydrolysis of esters. Amino acids correspond to those in PGA. (a) In the accepted mechanism for hydrolysis of esters, the catalytic serine (SerB1) attacks the ester once it binds in the active site. This attack forms the tetrahedral intermediate marked 1. Hydrogen bonds from two amide N-H's stabilize the oxyanion in this intermediate. Collapse of tetrahedral intermediate 1 releases the alcohol and forms an acyl enzyme intermediate. Attack of water on the acyl enzyme yields tetrahedral intermediate 2. Collapse releases the acid and regenerates the free enzyme. (b) A phosphonate mimics the transition states for formation and collapse of tetrahedral intermediate 1. Four hydrogen bonds, marked a–d, stabilize the charges. To be judged catalytically competent, the minimized structures must contain all four hydrogen bonds.

tion.<sup>35</sup> The crystal structure of the *p*-nitrophenylacetic acid/PGA complex solved by Done et al. was retrieved from the Brookhaven Protein Data Bank<sup>36</sup> (entry code 1ajn).

Using the Biopolymer module of Sybyl, hydrogen atoms were added to the unfilled valences of the amino acids. Histidines were uncharged, aspartates and glutamates were negatively charged, and arginines and lysines were positively charged. The inhibitor found in the crystal structure was considered as a template to select a trial conformation of the phosphonates (*R*)-**1**, (*S*)-**1**, (*R*)-**3**, and (*S*)-**3**. Docking of phosphonates (*R*)-**1**, (*S*)-**1**, (*R*)-**3**, and (*S*)-**3** into the PGA active site was carried out in two steps. First, we linked the phosphorus covalently to the O $\gamma$  of SerB1. Then, we identified a low-energy conformation of these compounds superimposable on the experimentally determined bioactive conformation of the PGA inhibitor *p*-nitrophenylacetic acid by manual adjustment of the torsion angles about the P–C<sub>1</sub>, C<sub>1</sub>–B<sub>2</sub> and B<sub>2</sub>–C<sub>3</sub> rotatable bonds (see Figures 4 for atom labeling). The overlay on *p*-nitrophenylacetic acid was performed by minimizing the root-mean-square distance between the centroids of aromatic rings and the COO<sup>−</sup>/POO<sup>−</sup> moieties. The resulting complexes were geometry-optimized by keeping fixed the coordinates of the protein backbone. Energy minimization proceeded in two stages: first, 1000 iterations of steepest descent algorithm and second, 1000 iterations of conjugate gradients algorithm until the rms deviation reached 0.005 Å mol<sup>−1</sup>. Water molecules and the substrate were not constrained through any of the minimization cycles.

The geometry-optimized structures were then used as the starting point for subsequent 200-ps molecular dynamics simula-

Table 2. Influence of Solute Structure on Hydrolysis Rate and Enantioselectivity<sup>a</sup>

substrate	<i>C</i> (%)	RSD (%)	ee <sup>b</sup> (%)	<i>E</i>
<b>1</b>	50.6	2.97	81.1 ( <i>S</i> )	23
<b>2</b>	5.4	0.46	39.0 ( <i>S</i> )	2.3
<b>3</b>	47.9	2.75	>99.9 ( <i>S</i> )	>200
<b>4</b>	19.7	4.8	4.3 ( <i>S</i> )	1.1
<b>5</b>	6.7	2.2	66.4 ( <i>S</i> )	5.3
<b>6</b>	10.5	0.64	38.2 ( <i>S</i> )	2.3
<b>7</b>	46.7	0.73	82.9 ( <i>S</i> )	23
<b>8</b>	28.2	0.42	17.1 ( <i>S</i> )	1.5
<b>9</b>	22.7	0.25	85.3 ( <i>S</i> )	15

<sup>a</sup> Reactor B. *C*, conversion (%); ee, enantiomeric excess (%); *E*, enantioselectivity; RSD, experimental error ( $n = 2$ ). See text for experimental details. <sup>b</sup> Fast reacted enantiomer.

tion, during which the protein backbone atoms were constrained as done in the previous step. A time step of 1 fs and a nonbonded pair list updated every 25 fs were used for the molecular dynamics simulations. The temperature was maintained at 300 K using the Berendsen algorithm with a 0.2-ps coupling constant. An average structure was calculated from the last 100-ps trajectory and energy-minimized using the steepest descent and conjugate gradient methods as specified above.

## RESULTS AND DISCUSSION

A chromatographic bioreactor based on PGA immobilized on monolithic support was developed in order to investigate the hydrolytic activity of PGA toward a series of 2-aryloxyalkanoic acid methyl esters and isosteric analogues, whose chemical structures are reported in Table 1. We decided to use monolithic supports because they are characterized by an almost complete lack of diffusion resistance during mass transfer; thus, they represent

(35) Weiner, S. J.; Kollman, P. A.; Case, D. A.; Singh, U. C.; Ghio, C.; Alagona, G.; Profeta, S., Jr.; Weiner, P. *J. Am. Chem. Soc.* **1984**, *106*, 765–784.

(36) Bernstein, F. C.; Koetzle, T. F.; Williams, G. J. B.; Meyer, E. F., Jr.; Brice, M. D.; Rodgers, J. R.; Kennard, O.; Shimanouchi, T.; Tasumi, T. *J. Mol. Biol.* **1977**, *112*, 535–542.

ideal materials for the immobilization of enzymes and fast conversion of substrates. Moreover, the large throughpores of monolithic materials allow high-speed analysis and low back pressures and consequently enable the coupling of the enzymatic column with the analytical column by means of a switching valve. The column-switching device was used to calculate the rate of substrate conversion ( $C$ ) and to collect the product whose enantiomeric excess ( $ee$ ) was calculated off-line for the determination of enantioselectivity ( $E$ ). The  $C$  and  $ee$  values together with  $E$ , calculated from the chromatographic data, are reported in Table 2.

High reaction rates ( $C > 40\%$ ) and enantioselectivity ( $ee > 80\%$ ) were obtained for **1**, **3**, and **7**; **1** and **7** are characterized by a methyl group in the  $\alpha$ -position while **3** presents a second aromatic ring on the asymmetric carbon. For this compound, a cleavage greater than 99.9% of the (*S*)-ester, corresponding to 47.9% conversion of the racemic ester, was observed. It is interesting to remark that a change of the substituent on the  $\alpha$ -position from a methyl (analyte **1**) to an ethyl (analyte **2**) group led to a dramatic reduction in the conversion rate and  $E$ .

The substituent on the aromatic ring (see **1** and **7–9**) seems to play a role in the reaction rate and enantioselectivity. The compounds with the most hydrophobic and electron-withdrawing substituent (**1** and **7**, respectively) are the most rapidly hydrolyzed with a high  $ee$  value. The presence of the oxygen in the  $\alpha$ -position is also important for the catalytic activity, all the isomers (**4–6**) present a low conversion rate, a low  $ee$  value, or both in comparison with **1**.

To explain the results of PGA enantioselectivity toward the aryloxyalkanoic acid methyl esters **1–9**, we used computer modeling of enzyme–transition-state analogue complexes. The binding site of PGA has been found to consist of three major regions that are responsible for the hydrolysis reaction of the substrates by the enzyme:<sup>1,6,7</sup> the catalytic residue SerB1, the oxyanion hole (stabilizing the negative charge present on one of the oxygens of the tetrahedral intermediates by hydrogen bonding) formed by GlnB23, AlaB69, AsnB241, and a hydrophobic pocket that is able to accommodate hydrophobic groups. The first chemical step in PGA-catalyzed ester hydrolysis is the attack of the active site serine (SerB1) on the ester carbonyl forming a tetrahedral intermediate. Collapse of this tetrahedral intermediate releases the alcohol, Figure 4a. We assume that the transition state involved in the formation or collapse of this first tetrahedral intermediate defines the selectivity of PGA toward aryloxyalkanoic acid methyl esters **1–9**. To mimic this transition state, we used the phosphonates linked to PGA shown in Figure 4b. Indeed, researchers have shown that phosphonates mimic the transition state for ester hydrolysis well.<sup>37,38</sup>

The docking geometries of compounds (*R*)-**1** and (*S*)-**1** gave their respective tetrahedral intermediates without losing favorable van der Waals and electrostatic interactions inside the active site of PGA. As depicted in Figure 5a, where the superimposition of the two intermediates is shown, the oxygen anion of both the tetrahedral intermediates gave the frame of four hydrogen bond interactions with the oxyanion hole residues GlnB23, AlaB69, and

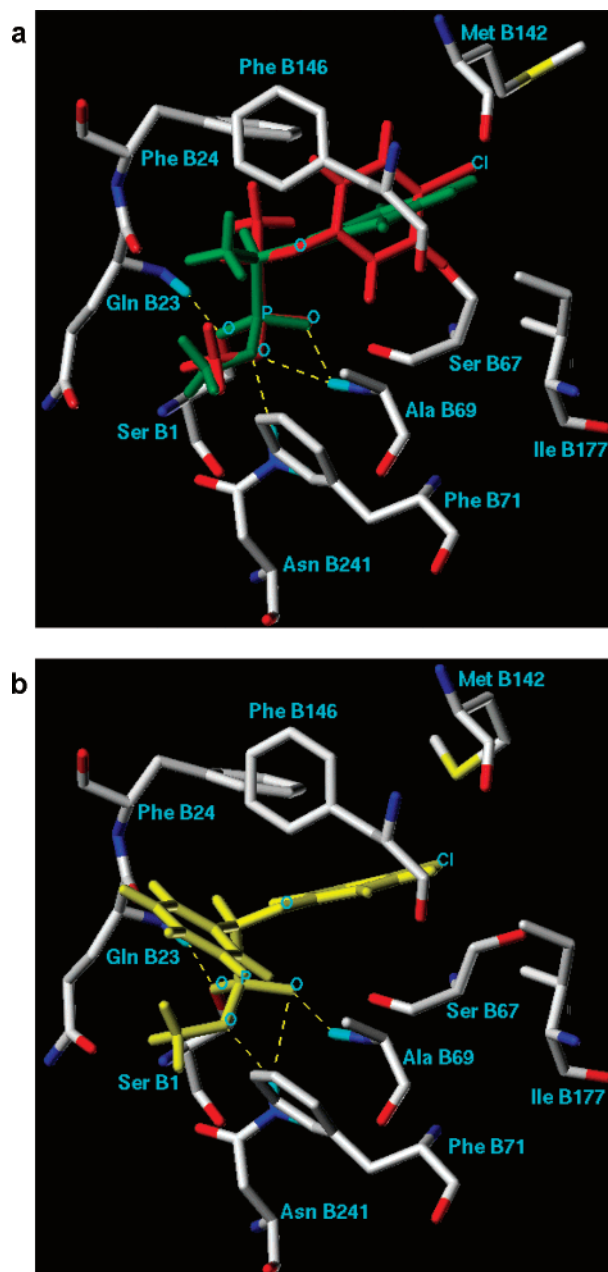


Figure 5. (a) Superimposition of the phosphonate transition-state analogues of (*R*)-**1** (red) and (*S*)-**1** (green), located at their proper respective three-dimensional position inside the active site of PGA. (b) Catalytically competent orientation of the phosphonate transition-state analogue of (*S*)-**3** (yellow) in the active site of PGA. Only amino acids located within 3 Å of the intermediates are displayed for the sake of clarity. Hydrogen-bonding interactions are depicted as dashed lines. Intermediates maintain all the catalytically essential hydrogen bonds identified in Figure 4b.

AsnB241. Moreover, in both intermediates, the *p*-chlorophenyl ring was located inside a hydrophobic pocket of the active site formed by the side chains of residues PheB24, ValB56, PheB57, AlaB69, SerB67, MetB142, TrpB154, and IleB177. In this pocket, the PheB24 side chain appeared in a suitable orientation for a  $\pi$ -stacking charge-transfer interaction with the *p*-chlorophenyl of the intermediates. Finally, it should be pointed out that in both cases the relevant intramolecular hydrogen bond interactions of PGA were not disrupted. However, a different scenario appeared

(37) Jacobs, J.; Schultz, P. G.; Sugawara, R.; Powell, M. J. *Am. Chem. Soc.* **1987**, *109*, 2174–2176.

(38) Hanson, J. E.; Kaplan, A. P.; Bartlett, P. A. *Biochemistry* **1989**, *28*, 6294–6305.

when the two structures were analyzed according to the position of the methyl substituent on the stereogenic center.

For the tetrahedral intermediate of (*R*)-**1**, the methyl group was located in a shallow pocket between PheB24, GlnB23, and ProB22, where bulkier groups could hardly be allocated. In contrast, the methyl group of (*S*)-**1** enantiomer was projected toward a hydrophobic pocket made up by the side chains of Phe71, Phe146, and Ala69, which leads to the opening of the active site. This pocket is medium-sized so that the methyl group fits properly in this configuration; however, it may preferentially accommodate planar  $\pi$ -electron systems to make favorable stacking and hydrophobic interactions. Accordingly, the phenyl group attached to the stereogenic center of (*S*)-**3**, showing an high reaction rate and enantioselectivity, was found to point toward this hydrophobic cavity at the opening of the active site and to contact PheB71 and PheB146 side chains favorably via a  $\pi$ -stacking and a T-shaped interaction, respectively (Figure 5b). Burley and Petsko have, in fact, shown that the aromatic–aromatic interactions are significant contributors to stabilization of both protein structure and ligand–protein complexes.<sup>39,40</sup> These interactions operate at centroid-to-centroid distances of 4.5–7.0 Å between interacting rings. The angle between the normal vectors of interacting aromatic rings is typically between 30° and 90°, producing a “T-shaped” or “edge-to-face” arrangement of interacting rings. Such interactions are reported to have energies between 1.0 and 2.0 kcal/mol.<sup>39</sup>

## CONCLUSIONS

PGA was successfully immobilized on a monolithic support, and the developed reactor combined with a switching valve was used as a highly efficient tool to study the enantioselectivity of ester hydrolyses catalyzed by PGA. The advantages of this chromatographic setup are the complete elimination of the downstream process, involving separation of product from the remaining substrate, the large decrease in enzyme and sample amount needed, and the precision by which *C* and ee can be calculated for the determination of *E*. Therefore, the described chromatographic system can be used to investigate the optimum reaction conditions, temperature, ionic strength, and pH, that influence enzyme enantioselectivity.

The hydrolysis of a series of 2-aryloxyalkanoic acid methyl esters and isosteric analogues was considered, and it has been observed that small structural modification, e.g., substituent in

the aromatic ring, atom in the  $\alpha$ -position to the stereogenic center, and type of substituent on the asymmetric carbon dramatically changed the conversion rate or the enantioselectivity of the reaction involving the selected substrates. The molecular modeling study supports the experimental observations on structure–property relationships of esters **1–9** processed by PGA. The reaction occurs well when a relatively small group such as methyl is present on the stereogenic center, preferentially in the *S* configuration. In the case of larger substituents, such as ethyl, the hydrolysis reaction is prevented, possibly due to steric hindrance within the active site. However, when a planar system is attached to the stereogenic center, the enzymatic hydrolysis reaction occurs again, since the complex is stabilized by favorable stacking interactions between the planar ring and PheB71 and PheB146 side chains.

As regards substituents on the aromatic ring, hydrophobic and electronic properties seem to play an important role in the enzymatic process control. The bromo derivative **7**, in fact, has a behavior similar to the chloro derivative **1**, as expected; the analogue **8** shows low conversion rate and enantioselectivity, possibly due to the poor hydrophobicity of the fluorine substituent. In the case of analogue **9**, on the contrary, a low conversion rate would be the result of the methyl group electron-donor properties that would weaken the  $\pi$ -stacking interaction formed between **9** and PheB24 aromatic rings. The isosteric replacement of the oxygen atom in the position  $\alpha$  to the stereogenic center (analogues **4–6**) affects the enzymatic hydrolysis too, producing lower conversion rate and enantioselectivity. One may speculate that the detrimental effect of the O/S/NH replacement originates from a less good accommodation of the *p*-chlorophenyl ring into the hydrophobic pocket of the enzymatic cavity due to the different stereoelectronic features of the isosteric substituents.

This information could expand the application of immobilized PGA as a chiral biocatalyst for the considered compounds and new processes. It could also be used to optimize the steric purity of products in the catalyzed transformation of chiral substrates.

## ACKNOWLEDGMENT

This work is supported by MURST (progetto: Analytical profile of drugs: advanced methodologies MM03104549\_002) and Galileo project.

Received for review June 26, 2002. Accepted November 4, 2002.

AC0204193

(39) Burely, S. K.; Petsko, G. A. *Science* **1985**, *229*, 23–28.

(40) Burely, S. K.; Petsko, G. A. *Adv. Protein Chem.* **1988**, *39*, 125–189.